ON CLUSTERS AND CLUSTERING, From Atoms to Fractals
P.J. Reynolds (Editor)

Two-dimensional Metallic Adlayers: Dispersion Versus Island Formation

Barry C. Bolding and Emily A. Carter*

13.1 Introduction

The study of thin film growth is of great importance in many areas of modern technology, and accurate models for describing thin film morphology is an active area of research. At low coverages, such morphology begins with cluster growth. Both Monte Carlo (MC) and molecular dynamics (MD) methods have been employed to study the mechanisms and morphology of such growth. The most commonly used methods involve some variation of the "solid on solid" (SOS)[1, 2] model, which can be studied by a lattice-gas MC technique. This approach is applicable to crystal and thin film growth of lattice-matched substrates and adlayers. The term lattice-matched refers to systems in which the substrate and adlayer intrinsically prefer identical lattice constants and symmetries. This model has been instrumental in understanding important processes such as surface roughening[1] and molecular beam epitaxial growth.[2] Lattice-matched systems have also been studied using MD methods[3] in order to examine the dynamics occurring within the adsorbed layer.

The growth of thin films that are lattice-mismatched with the substrate (i.e., where the substrate and adlayers prefer the *same* symmetries but have *different* lattice constants) have only been studied very recently. MC and MD methods have been used to examine a two-dimensional system with varying percentages of lattice mismatch in order to determine the range of lattice mismatches for which either commensurate or defective growth would occur.[4, 5] Metal-on-metal systems (Rh/Ag(100), Au/Ag(110) and Au/Cu(100)) have been investigated using corrected effective-medium potentials;[6, 7] and embedded-atom[8] (EAM) potentials for Cu on Ni(100).[9] The dynamics of adsorbates on such surfaces has also been examined, using a Lennard-Jones interaction[10] for the substrate and the adlayer. Recently, a discrete-lattice Monte Carlo model for lattice-mismatched thin film growth has also been proposed.[11]

The next level of complexity in thin film growth involves films with different preferred symmetries than the substrate. A variety of experiments have demonstrated the uniqueness of this type of growth. The unusual nature of such films is illustrated e.g. in experiments depositing thin layers of Pd (an fcc transition metal) onto W(110),[12] Nb(110) and Ta(110)[13–18] substrates (all bcc transition metals); and in experiments depositing the close-packed metals Co and Ni onto a bcc Mo(110) substrate.[19] Structural, thermodynamic and chemisorptive

*Department of Chemistry and Biochemistry University of California, Los Angeles, CA 90024-1569, USA.

properties for these systems are quite complex, and are extremely sensitive to coverage, temperature, and preparation method.

In this chapter, we examine the growth mechanism and structures formed in a model system involving an fcc metal (Pd) deposited onto a bcc(110) substrate at low coverages. The goal is to discern the structure of the film as it begins to grow, and to understand the physical reasons for the type of growth observed. In particular, we concern ourselves here with the submonolayer regime, in order to study island growth at a lattice-mismatched interface. These islands will ultimately determine the structural fate of the interface, that is whether it will be smooth or rough, commensurate or incommensurate, ordered or disordered. In the regime of low coverages, the adlayer is found to grow pseudomorphically (in sites which are a continuation of the underlying substrate lattice), both experimentally (for Pd on Ta(110)[14, 18] and Nb(110)[14, 20, 17]) and theoretically.[21, 22] This results from the potential energy corrugation induced by the substrate. This pseudomorphic growth, however, induces an internal strain within the adlayer that affects its structure and subsequent growth preferences. No additional information about the microscopic structure of the submonolayer film has been obtained from experiments; the calculations presented below are designed to provide a more detailed view of the metal adlayer and its growth mechanisms.

13.2 Model

13.2.1 Description

Since the fundamental nature of the interactions between a bcc metal and an fcc metal are not well understood, the model we describe assumes fcc-like interactions among the atoms adsorbing at the interface, while the substrate remains fixed in a bcc(110) configuration. The adlayer/substrate system is simulated using the EAM potential for Pd, developed by Foiles, Baskes and Daw,[23] which has been fit to bulk experimental data. In this potential, the total energy is expressed as a sum of an embedding energy $F_i(\rho)$, that represents the energy gained by embedding an atom i into a background electron density ρ, and a short-range repulsive term $\phi(R_{ij})$, which represents the core-core repulsions. Thus,

$$E_{\text{tot}} = \sum_i F_i(\rho) + \frac{1}{2}\sum_{i \neq j} \phi_{ij}(R_{ij}). \tag{13.1}$$

The total electron density at the position of atom i is found by a superposition of atomic electron densities from the other atoms in the system,

$$\rho = \sum_{j \neq i} \rho_j(R_{ij}). \tag{13.2}$$

Recently, potentials of this form have been used to study fcc(111)/fcc(111) interfaces,[24] elastic properties of thin slabs[25] and the structure of fcc thin metal films on fcc substrates.[6, 7] The results of these studies substantiate the use of the EAM potential for thin films. In addition to such fcc potentials, several EAM potentials have recently been developed for pure

bcc metals, including Nb,[26–29] but no potentials currently exist for describing an fcc-bcc interaction. The underlying character of this interaction has yet to be studied. This will require first-principles quantum mechanical calculations of mixed-metal systems to provide such understanding.[30]

Continuing with the model, the bcc substrate is created by placing fixed Pd atoms at bcc(110) lattice sites with a lattice constant of 3.31Å, mimicking the bcc metals Ta and Nb with their nearly identical lattice constants (3.30Å and 3.31Å). Using the Pd EAM potential for these fixed lattice sites sets up a corrugation potential periodicity similar to that of the real Nb or Ta substrates. The rigid-lattice approximation for the substrate still allows adatoms to move under the influence of the adatom-substrate and adatom-adatom interactions. These adatom-substrate interactions are actually quite reasonable, since the Pd desorption energy from this surface is close to the measured value[18] [3.9 (theory) versus 4.2 eV/adatom (experiment)], lending further credence to the use of the EAM potential to study surface phenomena. The corrugation potential induced by the substrate will favor pseudomorphic growth in the low coverage, low temperature limit. Since this potential has no heterogeneous terms to represent a mixed fcc/bcc interface, the model will yield structural information driven purely by the lattice mismatch between the preferred bulk structures of the two metals (Pd and Nb or Ta). Thus, if experiments for systems such as Pd/W(110), Pd/Nb(110), Pd/Ta(110) and Co/Mo(110) yield similar behavior, then one can infer that lattice strain effects provide the dominant driving forces for determining the observed structures.

13.2.2 Implementation

Four fixed layers of this bcc(110) structure in a two-dimensional periodic slab simulate the substrate. The periodic slab used contains 14 × 14 bcc(110) surface unit cells, giving it dimensions of 65.53Å × 46.34Å and 392 atoms/substrate-layer.

The results we will discuss were obtained by several Monte Carlo (MC) methods. Unless otherwise stated, the temperature is 500 K. In one method, adatoms are placed randomly in a slab 0.4Å thick and centered 2.0Å above the top fixed layer. The adatoms equilibrate for up to 50,000 MC steps/adatom. They may move by various jump distances, between 0.3Å and 2.8Å, to facilitate equilibration. For submonolayer coverages, this always results in a pseudomorphic structure. To test the degree of equilibration an alternative simple jump method may be used. The adatoms are allowed two types of displacements. If most jumps are short, this allows local vibrational equilibration and high acceptance ratios. On every fifth step, say, a long jump may be attempted. The long jump consists of picking an adatom at random and attempting a jump to a randomly chosen, empty, pseudomorphic site. The acceptance ratio for the long jump will be quite low, but this combined jump method allows faster equilibration than simple random walk methods. In the work we describe, the short jump displacement was chosen such that there were $\sim$ 10 accepted short jumps for each accepted long jump for each particle. Comparison of these two equilibration methods leads to confidence that the system has in fact reached equilibrium. Another method for forming the adlayer is MC vapor deposition. For this type of simulation, particles are deposited randomly on the surface, approximately 2Å above the equilibrium position for the adlayer. To allow time for equilibration, one particle is added to the system fairly infrequently. We have chosen

a rate of approximately every 200,000 MC steps. Once a given coverage is obtained, the entire adlayer is further equilibrated as described above. Once equilibrated, the system must be brought into local minimum energy configurations via either (or both) slow stepwise cooling (e.g., with 100 K intervals) or fast quenches, in order to analyze the underlying structural features.

13.3 Results

13.3.1 Static Lattice Calculations

In order to analyze the mechanisms involved in adlayer growth for coverages less that one monolayer (ML), we describe several specific static lattice calculations. In the limit of zero coverage, the barriers to diffusion across the substrate surface are of interest (see Fig. 13.1). To study the barriers, an adatom may be moved in increments across the surface in the desired direction. We chose at each x and y position to optimize the z position of the adatom by steepest descent energy minimization[31] (with the substrate fixed). This gives the minimum energy needed to move along the specified path. We caution that such barriers must be considered in terms of qualitative trends rather than accurate absolute values, since an empirical interaction potential has been employed. Nevertheless, the reasonable accuracy of the desorption energy when compared to experiment suggests that the energetics predicted from this model may be correct. However, we will only draw qualitative conclusions in what follows.

For adatom diffusion across a substrate atom (i.e., from $F \rightarrow H$ in Fig. 13.1), a barrier of E_d = 1.08 eV is encountered. The adatom traverses a path that must rise 0.47Å higher than the equilibrium position of the pseudomorphic adsite as it passes directly above the substrate atom. For diffusion that avoids crossing directly above a substrate atom (e.g., $F \rightarrow G$ in Fig. 13.1), the barrier is only E_d = 0.41 eV and the adatom rises only 0.18Å. This barrier is an upper bound to the actual barrier for this model, since the surface is not allowed to respond to the movement of the adatom. Thus we expect $E_d < 0.41$ eV, indicating that diffusion via bridging sites ($F \rightarrow G$) may occur readily at very low coverages, even at room temperature. Preferred diffusion along high-coordination sites makes sense physically, since metal-metal bonds are retained relative to the situation where diffusion involves passing over a one-fold site ($F \rightarrow H$).

For intermediate coverages, as two-dimensional bcc islands begin to grow, several mechanisms exist by which adlayer growth may proceed. First, an atom can land on the substrate surface far from an island, then perhaps diffuse toward an island, and finally attach to or migrate around the island. Second, an atom can land on top of an existing island, then diffuse to the edge and fall down onto the substrate, thus causing the island to grow in two dimensions. If the rate of diffusion of this second layer atom is slow, or the island size is large and the rate of deposition of atoms is rapid, then three-dimensional clustering may occur. Third, an atom can land on top of an island and be drawn into the first layer in the middle of the island, pushing the surrounding atoms outward. This mode of growth may be accessible because the adlayer is growing in a highly strained structure, with a density much lower than that preferred by bulk Pd. It therefore may be possible for an atom in the second adlayer to push into an interstitial site in the first adlayer.

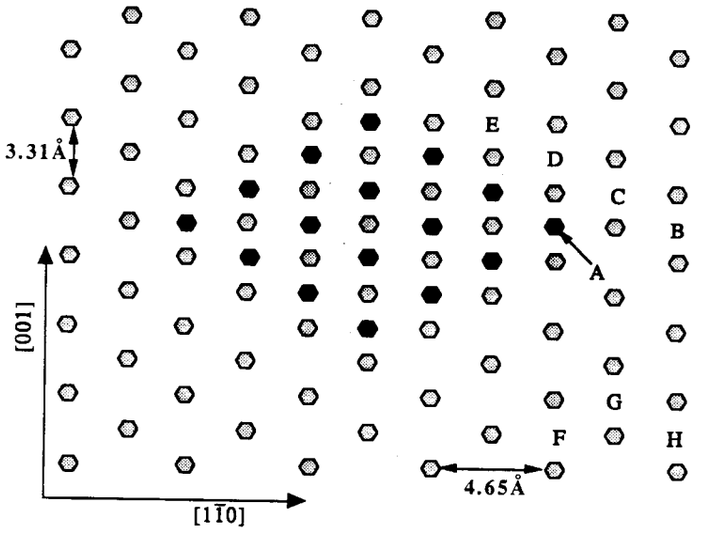

Figure 13.1: The geometries of the bcc(110) surface with a fifteen atom pseudomorphic cluster. The grey and black hexagons represent substrate atoms and adatoms, respectively. The lattice positions A-H are referred to in the text.

In order to study these alternative growth modes, one must examine the potential energy surface associated with each pathway. Migration of an atom near an adlayer island is shown in Fig. 13.1. The adatom at position A (to which the arrow points) was moved to the positions labeled B, C, D and E. At each position along the path, the z coordinate of the moving atoms was optimized by steepest descent energy minimization. The results are shown in Table 13.1. We see that diffusion away from an island is thermodynamically unfavorable ($A \rightarrow B$ or $A \rightarrow C$) by 0.73 eV, while diffusion along the corner ($A \rightarrow D$) is more favorable, only 0.33 eV uphill. The diffusion barriers suggest that diffusion around edges may proceed via initial movement away from the island ($E_b(A \rightarrow C)$ = 1.03 eV) and then movement back toward the island ($E_b(C \rightarrow D)$ = 0.32 eV), in order to avoid crossing over an atop site (as in $A \rightarrow D$ directly). Diffusion along the side of an inland has a very low barrier ($E_b(D \rightarrow E)$ = 0.24 eV). These results indicate that reorganization of an island is relatively facile. However, an atom near an island that is diffusing along the same paths as an isolated adatom (i.e. $A \rightarrow B$ versus $F \rightarrow H$ and $A \rightarrow C$ versus $F \rightarrow G$) experiences substantially larger barriers (see Table 13.1) because of the attractive interactions that act to prevent the island from dispersing. Thus, isolated adatom diffusion across interstitial sites, along with addition to and migration around the island ($C \rightarrow D$ and $D \rightarrow E$) are the most favorable diffusion pathways. Fission of an island of metal atoms is difficult. Thus, growth and reshaping of the island is preferred over island disintegration. These observations are similar to those found for Lennard-Jones simulations of lattice-mismatched thin film growth.[10]

Table 13.1: The initial, barrier, and final energies (E_i,E_b,E_f, respectively) and adatom positions (z_i, z_b and z_f) for the migration paths shown in Fig. 13.1. The positions are given in Å above the topmost fixed layer, in the surface normal direction. The zero of energy is taken to be that of an atom in site A, except for $F \rightarrow H$ and $F \rightarrow G$ where the zero of energy is that of an isolated pseudomorphic adatom on the surface.

Migration Path	E_i(eV)	E_b(eV)	E_f(eV)	z_i(Å)	z_b(Å)	z_f(Å)
$A \rightarrow B$	0.00	1.81	0.73	1.87	2.04	1.70
$A \rightarrow C$	0.00	1.03	0.73	1.87	1.82	1.66
$A \rightarrow D$	0.00	1.14	0.33	1.87	2.19	1.71
$C \rightarrow D$	0.73	1.05	0.33	1.66	1.81	1.71
$D \rightarrow E$	0.33	0.57	0.20	1.71	1.88	1.76
$F \rightarrow H$	0.00	1.08	0.00	1.63	2.10	1.63
$F \rightarrow G$	0.00	0.41	0.00	1.63	1.81	1.63

As the coverage increases, and hence the two-dimensional island size increases, modes two and three (where an atom lands on top of an island) will compete. Mode two will experience the same barriers as an isolated adatom in our model, since the interactions are all homogeneous. In other words, diffusion may proceed with a barrier of 0.41 eV, until it reaches the edge of the cluster. At that point, it can drop off into the first layer. While this a viable mechanism, we find mode three, where the atom is drawn into the first layer, to be more accessible, especially at higher temperatures. We see this by studying the energy barrier to incorporation of an adatom into the first adlayer of an 18-atom island (shown in Fig. 13.2). Consider two possible approaches for an incoming Pd atom onto the island: (*i*) directly above a substrate atom (*A*) and (*ii*) in an interstitial region between two adatoms in the island (*B*). By lowering the incoming atom into the island in 0.1Å increments and reoptimizing the positions of all of the other atoms in the island by steepest descent, the two potential energy curves shown in Fig. 13.3 were obtained. The incoming atom is found to be stable in a second layer pseudomorphic position at *A*. Ultimately, however, a lower energy can be achieved if the adatom can move from *A* into the interstitial site *B* while being pulled down into the first layer. This diffusion from *A* to *B* again involves a barrier of 0.41 eV (assuming movement in the plane parallel to the surface and then downward), but may be considerably smaller if the cluster has time to relax and vibrational motion within the cluster is sufficiently large. Mode three is therefore a reasonable mechanism for island growth under conditions where the island can respond (i.e., at high temperatures). This is consistent with studies of thin film growth at 500 K, where molecular dynamics simulations indicated that incorporation of a second layer atom into a full pseudomorphic monolayer occurs in less than one picosecond.[21] However, if an incoming particle has sufficiently small kinetic energy and the substrate is cold, then it is possible to become trapped in the second layer position, leading to three-dimensional pseudomorphic growth at low temperatures.[22] Recent methods using a rare-gas buffer layer between the substrate and adlayer are promising for such cold metal atom depositions in a single monolayer.[32] More details can be found in the following chapter.

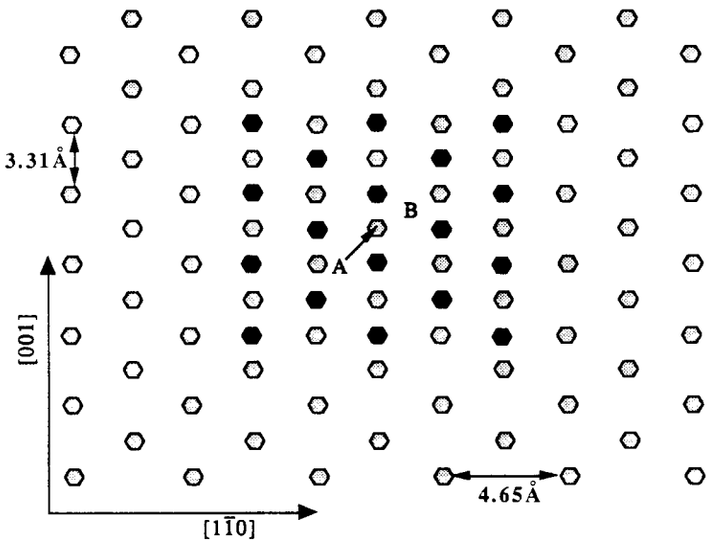

Figure 13.2: The geometries of the bcc(110) surface with an eighteen atom pseudomorphic cluster used to find the potential energy for embedding an atom into the first layer. The grey and black hexagons represent substrate atoms and adatoms, respectively. The embedding positions *A* and *B* are referred to in the text.

13.3.2 Monte Carlo Simulations

Given these possible growth and diffusion mechanisms, it is important to investigate the actual equilibrium structures obtained at submonolayer coverages within this model. At coverages of Θ_{Pd} = 0.25 and 0.50 ML, MC simulations (at both 500 K and 1000 K) reveal a fully commensurate structure with variously-sized islands. The Pd-Pd distances are slightly contracted (2.67Å) from the ideal, nearest-neighbor, bcc substrate distance of 2.86Å in order to maximize bonding. This contraction appears to be more pronounced for atoms bonded to the edges than the center of islands. In addition, the islands are elongated and preferentially oriented parallel to the bcc[001] direction. At Θ_{Pd} = 0.75 ML, the commensurate adlayer becomes a single extended island, percolating in the bcc[001] direction. These clusters however are not percolation clusters, but are compact structures. Figs. 13.4 and 13.5 show the adlayer structures at 0.50 and 0.75 ML, respectively. The single island found at 0.75 ML is a column propagating along the [001] azimuth. Considering our periodic boundary conditions, this indicates channels devoid of adatoms may exist on the extended surface. The reason for the preferred direction is easily understood in terms of maximizing the coordination number of the adatoms. The next-nearest-neighbor distance is 3.31Å in the [001] direction, whereas it is 4.68Å in the [$\bar{1}$10] direction. The energetics will thus tend to favor growth along [001]. Furthermore, the nearest-neighbor bcc distance of 2.86Å favors a zig-zag structure, where atoms

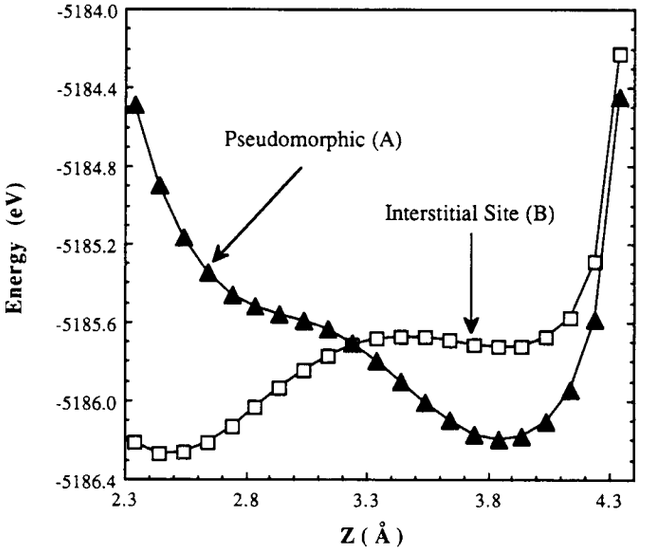

Figure 13.3: The potential energy curves for embedding an adatom into the adatom cluster shown in Fig. 13.2. The origin of z is taken to be the topmost fixed substrate layer. This figure indicates that a second layer position above the island is stable (z = 3.85Å) but a lower energy can be obtained at the interstitial site, within the first layer(z = 2.45Å).

add to the island along the $[\bar{1}11]$ direction or the $[1\bar{1}1]$ direction (see Fig. 13.6), which maximizes the nearest-neighbor bonds of 2.86Å. The zig-zag structure occurs instead of growth along only the $[\bar{1}11]$ or $[1\bar{1}1]$ direction because, while the latter maximizes the total number of nearest-neighbor bonds, only the former also maximizes the total number of nearest plus next-nearest-neighbor bonds. Thus the preferred growth is a zig-zag of rhombi with overall growth along the [001] direction. This zig-zag structure is lower in energy than a chain along the $[1\bar{1}1]$ direction by 0.015 eV/adatom (at 0 K).

Finally, we discuss two special adlayer structures that we investigated for each coverage (Θ_{Pd} = 0.25, 0.50, 0.75, 1.00 ML). These are single bcc islands ($Pd_{bcc}(110)$) and single fcc(111) islands where the orientation of the island with respect to the substrate is optimized. A single $Pd_{bcc}(110)$ island is found to be lower in energy than all other structures for all coverages up to 1.0 bcc ML, consistent with the predicted low diffusion barrier for isolated atoms, which allows aggregation to occur. The fcc islands always were found to be unstable at 500 K, transforming to bcc islands, although sometimes with small fcc regions in their interior. For instance, at 0.50 ML, the minimum energy configuration of a single bcc island is 0.04 eV/adatom more stable than an equilibrated, random island network, and 0.35 eV/adatom more stable than a single fcc island. Thus, surface corrugation dominates the structure of islands, at least at the temperatures we examined.

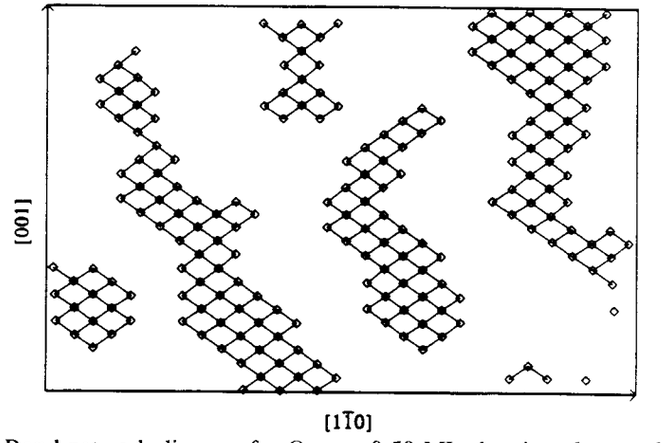

Figure 13.4: Bond network diagram for Θ_{Pd} = 0.50 ML showing elongated island structures observed in the simulations. Bonds are drawn for all interatomic distances closer than 3.1Å. For reference, a perfect bcc(110) surface would be depicted as a surface of periodically replicated rhombi. The structure shown is quenched to 0.1 K from a 500 K equilibration.

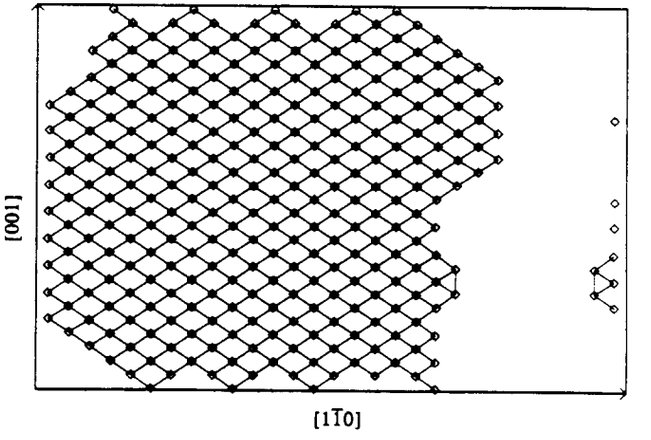

Figure 13.5: Bond network diagram for Θ_{Pd} = 0.75 ML showing the percolated single island in the [001] direction that will lead to channel-like features. Bonds are drawn for all interatomic distances closer than 3.1Å. The structure shown is quenched to 0.1 K from a 500 K equilibration.

13.4 Summary and Conclusions

The mechanisms and structures found for strained metal overlayers should be helpful in understanding actual fcc/bcc(110) interfaces. Small diffusion barriers for movement toward and

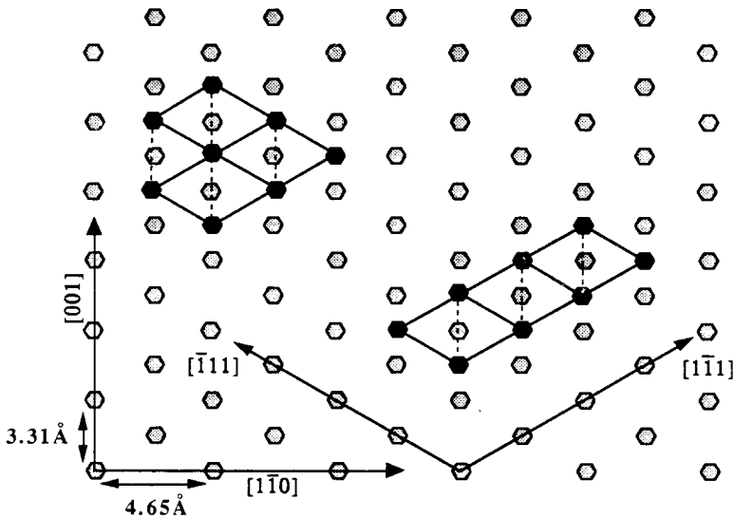

Figure 13.6: The geometries of two 8-atom pseudomorphic clusters on a bcc(110) surface. Both clusters have 10 near-neighbor interactions, but the zig-zag cluster has one additional next-nearest-neighbor interaction. The energy difference between the two clusters is discussed in the text.

along island edges, as well as for isolated adatoms contrasts with much larger barriers for movement of atoms away from an island. Taken together, the energetics favor aggregation and reshaping of islands in a zig-zag pattern of rhombi along the [001] direction, thereby maximizing the nearest and next-nearest-neighbor attractions. These elongated anisotropic islands and channels found at 0.50 ML and 0.75 ML have not yet been observed directly in experiments. Nevertheless, Ion Scattering Spectroscopy (ISS) should be able to detect such structures. Furthermore, the contraction of the Pd-Pd near-neighbor distances (by 0.19Å) predicted for these coverages might be measurable with Surface-Extended X-Ray Absorption Fine Structure (SEXAFS) or Low Energy Electron Diffraction (LEED) methods.

The incorporation of a second layer adatom into the center of an island and subsequent outward relaxation of the island involves no barrier except for diffusion on top of the island. Thus, for low temperatures where the diffusion barrier cannot be overcome, the growth is expected to be three dimensional and pseudomorphic, consistent with earlier studies.[22] At high temperatures, the 0.41 eV diffusion barrier can be surmounted easily, with vibrational motion of the adlayer sufficient for outward relaxation of the island to occur. This allows ready incorporation of the additional atom into the first layer. Recent experimental work indicates that this island relaxation may be responsible for changes in LEED patterns for Co on Mo(110), when a vapor deposited submonolayer film of Co is allowed time to achieve equilibrium.[19]

The model presented here is the most realistic to date for lattice-mismatched island and thin film growth of materials with different preferred symmetries. It serves as an extremely important reference system for island and film growth in the case where the bcc substrate and fcc adlayer interactions are similar in nature. The consistency with which this model reproduces experimental results for higher coverage thin film growth[22] lends credence to its predictive ability for submonolayer coverages where, to date, little experimentally-determined data is available.

Acknowledgements

This work is supported by the Office of Naval Research. EAC also acknowledges a National Science Foundation Presidential Young Investigator Award and Camille and Henry Dreyfus Distinguished New Faculty Award. We thank Dr. Steven Foiles for providing the embedded atom potential data for Pd. Simulations were performed on an FPS 511 computer purchased through the Department of Defense University Research Instrumentation Program and augmented with funds from the Office of Naval Research.

References

1. J. D. Weeks and G. H. Gilmer, Adv. in Chem. Phys. **40**, 157 (1979).
2. S. Das Sarma, J. Vac. Sci. Technol. **A 8**, 2714 (1990).
3. S. M. Paik and S. Das Sarma, Surface Sci. **208**, L53 (1989).
4. B. W. Dodson and P. A. Taylor, Phys. Rev. B **34**, 2112 (1986).
5. P. A. Taylor and B. W. Dodson, Phys. Rev. B **36**, 1355 (1987).
6. T. J. Raeker, D. E. Sanders, and A. E. DePristo, J. Vac. Sci. Tech. **A 8**, 3531 (1990).
7. T. J. Raeker and A. E. DePristo, Surface Sci. **248**, 134 (1991).
8. M. S. Daw and M. I. Baskes, Phys. Rev. B **29**, 6443 (1984).
9. C. S. Murthy and B. M. Rice, Phys. Rev. B **41**, 3391 (1990).
10. S. M. Paik and S. Das Sarma, Surface Sci. **208**, L61 (1989).
11. D. A. Faux, G. Gaynor, C. L. Carson, C. K. Hall, and J. Bernholc, Phys. Rev. B **42**, 2914 (1990).
12. D. Prigge, W. Schlenk, and E. Bauer, Surface Sci. **123**, L698 (1982).
13. M. A. Pick, J. W. Davenport, M. Strongin, and G. J. Dienes, Phys. Rev. Lett. **41**, 286 (1979).
14. M. Strongin, M. El-Batanouny, and M. Pick, Phys. Rev. B **22**, 3126 (1980).
15. M. W. Ruckman, P. D. Johnson, and M. Strongin, Phys. Rev. B **31**, 3405 (1985).
16. M. W. Ruckman, V. Murgai, and M. Strongin, Phys. Rev. B **34**, 6759 (1986).
17. D. L. Neiman and B. E. Koel, "Surface Chemistry of Thin Palladium Films," in *Physical and Chemical Properties of Thin Metal Overlayers and Alloy Surfaces*, D. M. Zehner and D. W. Goodman, eds. (Materials Research Society, Pittsburgh, 1988).
18. B. E. Koel, R. Smith, and P. Berlowitz, Surface Sci. **231**, 325 (1990).
19. M. Tikhov and E. Bauer, Surface Sci. **232**, 73 (1990).
20. M. Sagurton, M. Strongin, F. Jona, and J. Colbert, Phys. Rev. B **28**, 4075 (1983).
21. B. C. Bolding and E. A. Carter, Phys. Rev. B **42**, 11380 (1990).

22. B. C. Bolding and E. A. Carter, Phys. Rev. B **44**, 3251 (1991).
23. S. M. Foiles, M. I. Baskes, and M. S. Daw, Phys. Rev. B **33**, 7983 (1986).
24. B. W. Dodson, Surface Sci. **184**, 1 (1987).
25. D. Wolf, Surface Sci. **225**, 117 (1990).
26. J. M. Eridon and S. Rao, "Derivation of Many-Body Potentials for Examining Defect Behavior in bcc Nb," in *Atomic Scale Calculations in Materials Science*, J. Tersoff, D. Vanderbilt, and V. Vitek, eds. (Materials Research Society, Pittsburgh, 1989).
27. J. M. Eridon and S. Rao, Phil. Mag. Lett. **59**, 31 (1989).
28. M. I. Haftel, T. D. Andreadis, J. V. Lill, and J. M. Eridon, Phys. Rev. B **42**, 11540 (1990).
29. J. B. Adams and S. M. Foiles, Phys. Rev. B **41**, 3316 (1990).
30. H. Wang and E. A. Carter, J. Am. Chem. Soc., *submitted.*
31. W. H. Press, B. P. Flannery, S. A. Teukolsky and W. Vetterling, *Numerical Recipes: The Art of Scientific Computing*, (Cambridge University Press, Cambridge, 1989).
32. J. H. Weaver and G. D. Waddill, Science **251**, 1444 (1991).